

3. Бусько В.Л., Лобатый А.А., Русак Л.В. Аналитическое моделирование дискретных систем с фазовым управлением // Доклады БГУИР, 2008 № 3 (33) с. 103-110.

4. Бусько В.Л., Лобатый А.А., Русак Л.В. Анализ вероятностных характеристик дискретных систем с фазовым управлением // Доклады БГУИР, 2008 № 8 (38) с. 93-99.

5. Методы оптимизации / под ред. В.С. Зарубин, А.П. Крищенко. – М.: Издательство МГТУ им. Н.Э.Баумана, 2003. – 440 с.

6. Синтез регуляторов систем автоматического управления / под ред. К.А. Пупков и Н.Д. Егупова. - М.: Издательство МГТУ им. Н.Э. Баумана, 2004.-616 с.

7. Соболев И.М. Точки, равномерно заполняющие многомерный куб.–М.: Знание, 1985.– 32 с.

8. Соболев И.М., Статников Р.Б. Выбор оптимальных параметров в задачах со многими критериями.– М.: Наука, 1981.– 193 с.

UDC 621.002

STRUCTURE DEVELOPMENT AND SIMULATION OF PLUG-IN HYBRID ELECTRIC VEHICLE

*M.Sc. ALEH MAROZKA, Associate professor YURY PETRENKO
Belarusian National Technical University*

Introduction

Electric-drive vehicles (EDVs) have gained attention, especially in the context of growing concerns about global warming and energy security aspects associated with road transport.

The main characteristic of EDVs is that the torque is supplied to the wheels by an electric motor that is powered either solely by a battery or in combination with an internal combustion engine (ICE). This covers hybrid electric vehicles (HEVs), battery electric vehicles (BEVs), and plug-in hybrid electric vehicles (PHEVs), but also photovoltaic electric vehicles (PVEVs) and fuel-cell vehicles (FCVs). [1]

So we initiated research work with a view to assess the economic impacts, engineering constraints and user needs of a future market penetration of those car technologies, with a focus on PHEVs.

As a starting step, we reviewed the literature and prepared this paper which provides a summary description of the technology aspects, the current

state of the research and development in the field. It also elaborates consistent sets of data about the vehicle technologies in view of the subsequent modeling work to undertake the assessment. The paper also identifies a series of areas where more data and assessment are needed.

General definitions

Battery Electric Vehicles refer to vehicles propelled solely by electric motors. The source of power stems from the chemical energy stored in battery packs which can be recharged on the electricity grid. The future of such vehicles strongly depends on the battery developments (performance and cost).

Plug-in Hybrid Electric Vehicles refer to vehicles that can use, independently or not, fuel and electricity, both of them rechargeable from external sources. PHEVs can be seen as an intermediate technology between BEVs and HEVs. It can indeed be considered as either a BEV supplemented with an internal combustion engine (ICE) to increase the

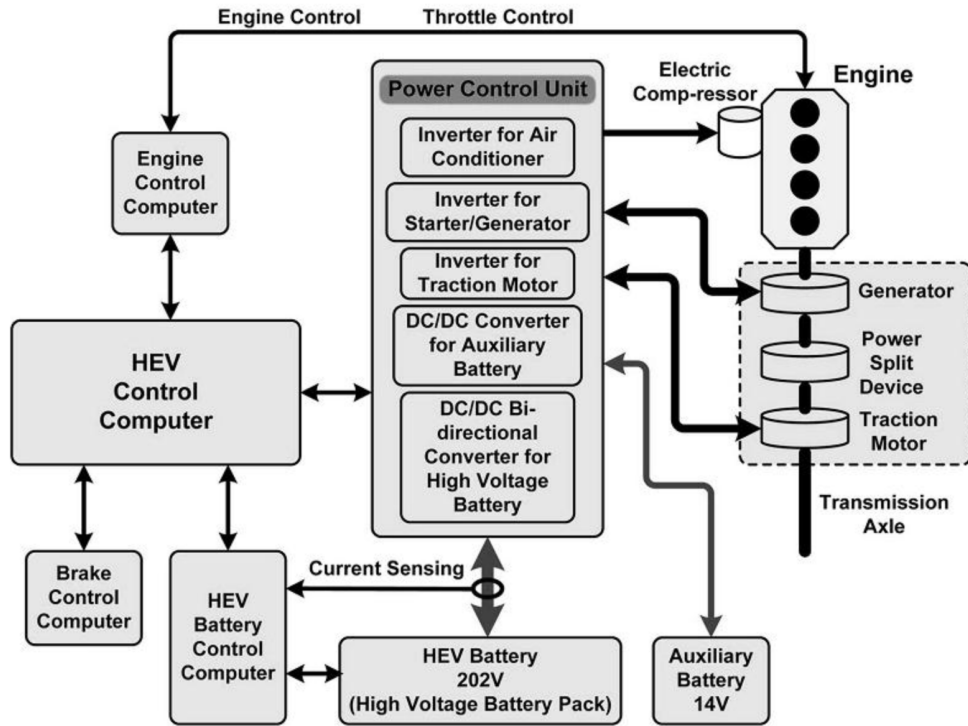


Fig. 2. Power control unit (Toyota Hybrid Synergy II).

inverter for the traction motor, a dc–dc converter for the auxiliary battery, and a dc–dc bidirectional converter for the high voltage battery. The goals of the U.S. Partnership for a New Generation of Vehicles for power electronics and electric machinery are quite challenging and are given in Table I.

Table 1. Technical Targets of Electric Machines (a) and Power Electronics (b) (Including Active Materials, Motor Gears and Housing)

(a)	
Characteristics	
Peak Power to Weight Ratio [kW/kg]	>1.3
Peak Power to Volume Ratio [kW/liter]	>5
Cost/Peak [\$ /kW]	<7
Efficiency (@10% to 100% of max. speed)	>93
Nominal Voltage [V]	325
Maximum Current [Arms]	400
(b)	
Characteristics	
Peak Power to Weight Ratio [kW/kg]	>12
Peak Power to Volume Ratio [kW/liter]	>12
Cost [\$ /kW]	<5
Efficiency [%]	97
Coolant Inlet Temperature [°C]	105
Lifetime [years]	15

To meet the requirements of the automotive environment, several technical challenges need to be overcome, and new developments are necessary, from the device level to the system level. [3,4]

A. Development and Research on Switches for High-Switching-Frequency, High-Power, and High-Temperature Applications

In [5] a liquid-cooled soft-switch module has been developed. The module integrates main IGBTs, MOSFETs, auxiliary IGBTs, and diodes with a capability of 400-A continuous current operation. The integration of these chips allows significant parasitic inductance and thermal resistance reduction. Using such a highly integrated liquid-cooled soft-switch module, a 55-kW three-phase soft-switching inverter was designed and assembled. The inverter efficiency was evaluated under both inductive load and motor-dynamometer load tests with coolant temperatures ranging from 25 °C to 90 °C. A double-chamber differential calorimeter was introduced for precision inverter efficiency measurement. The soft-switching inverter was successfully operated at various temperature and test conditions. The power meter measurement from 20% to 100% output consistently

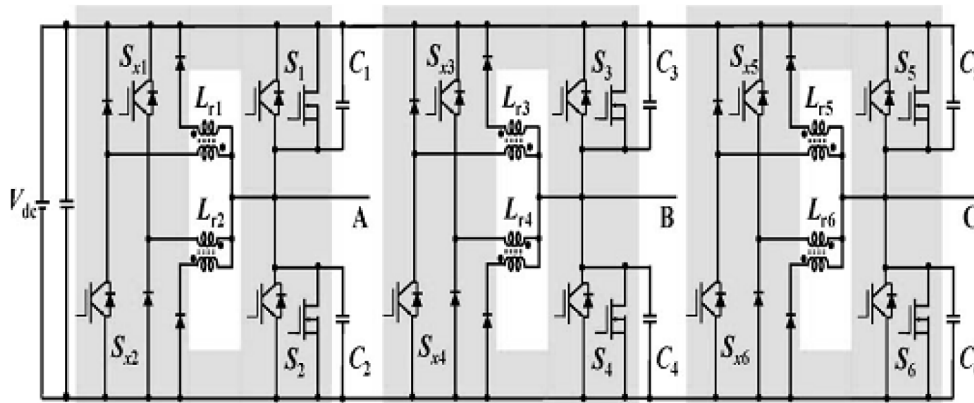


Fig. 3. Circuit Diagram of three-phase soft-switching-module-based inverter.

shows efficiency higher than 98% under different temperature conditions, and the peak efficiency with calorimeter measurement exceeds 99%.

The three-phase soft-switching inverter consisted of three identical soft-switching modules, which are shown in shaded area in Fig. 3. S1 to S6 are the hybrid main switches composed of paralleled IGBT and MOSFET devices. Sx1 to Sx6 are auxiliary IGBT switches. In each module, there are also four auxiliary diodes. All the devices have the voltage rating of 600 V. Lr1 to Lr6 are coupled magnetics with turns ratio of 1 : 1.35. C1 to C6 are resonant capacitors with a value of 100 nF.

B. Energy Storage System Technologies

Power electronics have revolutionized motor drives, bringing within the realm of possibility electric drive-trains with extremely high

performance. The motors themselves have been improved, offering higher reliability and better performance with reduced cost. Unfortunately, the weak link in the electric drivetrain development chain remains—energy storage. There are some advancements in energy storage device development which offer good promise in terms of energy density and power density, but none has the desired combination of all the following features: fast charging/discharging (high power density), large storage capacity (high energy density), low cost, and long life.

There are many potential methods of pairing a battery and ultra-capacitors (UC). Researchers [6] have considered a direct parallel connection of the two sources (Fig. 4a). This setup keeps the same voltage over both sources, which in turn limits the power delivered from the UC.

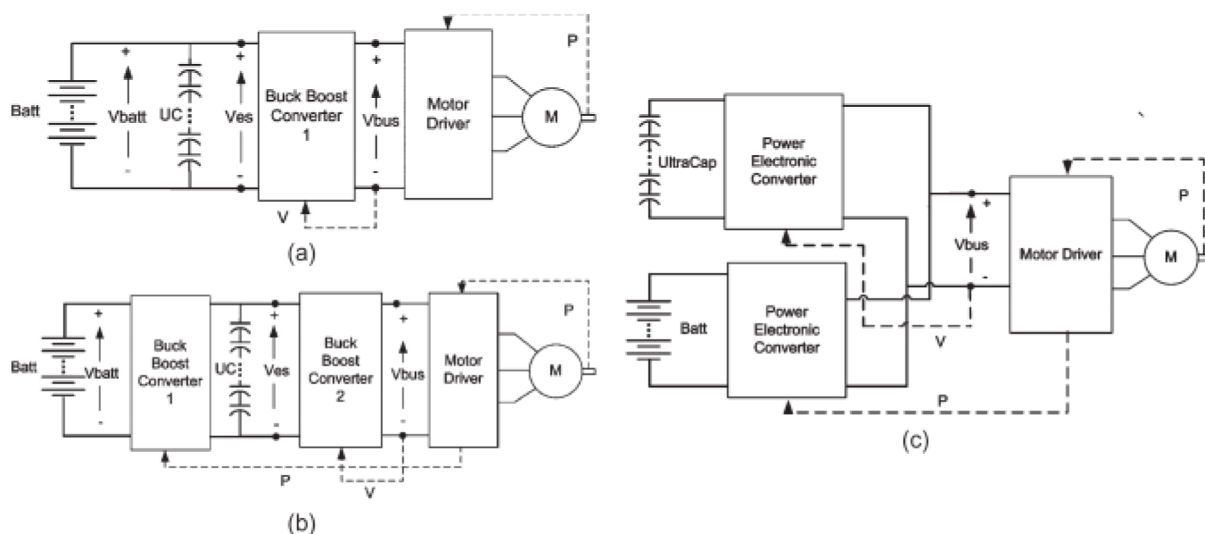


Fig. 4. Topology of the (a) passive parallel connection, (b) bidirectional dc/dc converter, (c) two-input bidirectional dc/dc converter.

Alternatively, a bidirectional dc/dc converter placed between the batteries and the UCs may be used (Fig. 4b). Buck-boost 1 controls the current output of the battery, while the UC supplies the remaining power requirement to the load. This system allows decoupling of the battery and UC voltages. However, there is a large voltage swing on the input to Buck-Boost 2, which reduces efficiency due to larger IR losses at low UC voltages.

Finally, some researchers [6], [7] have looked at using a two-input bidirectional dc/dc converter (Fig. 4c). This gives the highest flexibility and provides the same functionality as the bidirectional dc/dc converter. The two-input bidirectional converter topology is superior from both a stability and efficiency point of view due to the decoupling of the power-supplying paths. The stability is also improved since a failure of one source still allows the operation of the other.

Since no existing device is able to achieve all of the requirements of various vehicular applications, the concept of combining devices to obtain their best traits is considered.

D. Fault-Tolerant Topology

In [8] authors have reviewed the fault tolerant three-phase ac motor drive topologies that have been presented in the literature. An approach based on the fundamental inverter output space in terms of axis limits has been adopted as a basis to identify the potential performance limits of each of the topologies. From these limits, a fault power rating factor (FPRF) has been defined which normalizes the faulted system capacity to a standard three-phase inverter during normal unfaulted operation.

$$FPRF = \frac{\text{maximum kVA output during fault}}{\text{max. kVA output of std. unfaulted inverter}}.$$

To compare the relative cost of adding the fault tolerant capacity in each of the topologies, this paper has defined a SOCF which relates each circuit's weighted switch capacity to that of a standard three-phase inverter.

$$SOCF = \frac{\text{weighted kVA rating of all switches}}{\text{kVA rating of standard inverter switches}}.$$

After review of the alternative topologies and control methods makes it clear that there is significant cost associated with providing fault tolerant operation. All of the topologies require additional components in the form of silicon switches and/or fuses to provide this capacity in the presence of a fault that would otherwise not be present in a standard three-phase inverter drive.

Among the topologies and faults considered, key results include the following.

1) The switch-redundant topology provides the full post-fault current rating for both a single-switch short or single switch open fault at a modest cost increase (approximately 50%) and is a good candidate provided the midpoint of the dc link is available for use. Furthermore, this topology can be adapted to accommodate open phase faults with an additional TRIAC.

2) The double switch-redundant topology with a four terminal motor is fault tolerant to all four inverter faults considered: Single switch short-circuit, phase-leg short-circuit, single switch open-circuit, and single-phase open-circuit. It has a post-fault kVA delivery factor (FPRF) of 0.58.

3) The phase-redundant topology with a three terminal motor is fault tolerant to all four of the considered faults and has a FPRF value of 1.0. This superior solution also has the highest component cost of any fault tolerant topology at 233% of that of a standard inverter.

4) The use of single-phase units or cascaded inverters has the smallest cost penalty factor (SOCF) at 115% of the cost of a standard inverter but only provides fault tolerance to open phase faults. With the addition of TRIAC in each phase, this system is fault tolerant to single switch open, and short faults, and single-phase open-circuits. This increases the SOCF cost factor to 144% for a FPRF value of 0.58.

5) Four-leg inverters provide fault tolerance only to open phase or open switch faults at a

relatively high cost.

In conclusion, a careful assessment of the likelihood of each type of fault and the required post-fault capacity is necessary to determine which topology is best suited for each application.

E. Robust Sensorless Control and Low-Cost High-Temperature Magnets of Electric Propulsion Machine

Hybrid Vehicle Control System: The Hybrid Vehicle Control Unit (HV ECU) optimizes the power output and the torque of driving forces to reduce the fuel consumption and the pollutant of the exhaust gas. The optimal required driving power of the Internal Combustion Engine (ICE), motor-generators MG1 and MG2 is based on its inputs signals which are the gas pedal position, rotation speed of the drive shaft and gear shift lever position. Also the state of charge (SOC) of the battery pack and the temperature of the motor-generators have influence on the optimal driving power. Figure 5 shows a schematic diagram of the communication between the HV ECU and the other Hybrid Synergy Drive (HSD) devices. [9]

Induction Motor Dynamic Model:

A. Nomenclature

- $V_{ds} (V_{qs})$ d -axis (q -axis) stator voltages.
- $i_{ds} (i_{qs})$ d -axis (q -axis) stator currents.
- $\lambda_{dr} (\lambda_{qr})$ d -axis (q -axis) rotor flux linkages.
- T_L Load torque.

- $R_s (R_r)$ Stator (rotor) resistance.
- $L_s (L_r)$ Stator (rotor) inductance.
- L_m Magnetizing inductance.
- L_σ Leakage inductance ($L_\sigma = L_s - L_m^2/L_r$).
- $\omega_e (\omega_r)$ Stator (rotor) electrical speed.
- Ω Rotor speed (ω_r/p).
- ω_{sl} Slip frequency, $\omega_{sl} = \omega_e - \omega_r$.
- B Motor damping ratio.
- p Pole-pair number.

$$\begin{cases} k_1 = \frac{R_s}{L_\sigma} + \frac{R_r L_m^2}{L_r^2 L_\sigma}, & k_2 = \frac{R_r L_m}{L_r^2 L_\sigma}, & k_3 = \frac{L_m}{L_r L_\sigma}, \\ k_4 = \frac{R_r L_m}{L_r}, & k_5 = \frac{R_r}{L_r}, & k_6 = \frac{1}{L_\sigma}, & k_t = \frac{3}{2} p \frac{L_m}{L_r}. \end{cases}$$

Generally, dynamic modeling of an induction motor drive is based on rotating reference-frame theory and a linear technique. This motor drive consists of an induction motor, a bang–bang current-controlled pulse-width modulated inverter, a field-orientation mechanism, a coordinate translator and a speed controller. The electrical dynamics of an induction motor in the synchronously rotating reference frame (d – q axis) can be expressed by equations:

$$\frac{d}{dt} \begin{bmatrix} i_{ds} \\ i_{qs} \\ \lambda_{dr} \\ \lambda_{qr} \end{bmatrix} = \begin{bmatrix} -k_1 & \omega_e & k_2 & \omega_r k_3 \\ -\omega_e & -k_1 & -\omega_r k_3 & k_2 \\ k_4 & 0 & -k_5 & \omega_{sl} \\ 0 & k_4 & -\omega_{sl} & -k_5 \end{bmatrix} \begin{bmatrix} i_{ds} \\ i_{qs} \\ \lambda_{dr} \\ \lambda_{qr} \end{bmatrix} + k_6 \begin{bmatrix} V_{ds} \\ V_{qs} \\ 0 \\ 0 \end{bmatrix}$$

$$\frac{d\omega_r}{dt} = -\frac{B}{J}\omega_r - \frac{1}{J}(T_m - T_L)$$

$$T_m = k_t(\lambda_{dr} i_{qs} - \lambda_{qr} i_{ds}).$$

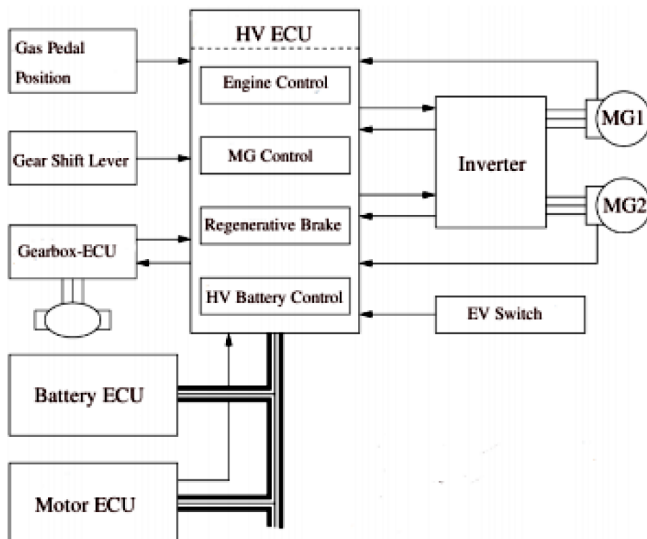


Fig.5. Diagram of the HSD communication system.

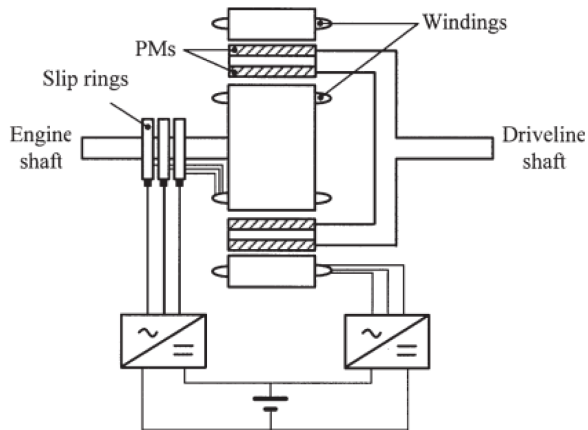


Fig. 6. Integrated PM BL EVT system.

mild HEVs, and the PM BL EVT (electric variable transmission) system for full HEVs. It is anticipated that the “totally brushless” configuration of the PM BL EVT systems will be a major research direction in the field of HEVs.

Modeling

MATLAB is widely used in academic and research institutions as well as industrial enterprises for complex systems simulation [11]. Mathematical model of PHEV was created on the base of official Matlab example [12,13]. Developed model shows a multi-domain simulation of a PHEV power train based on SimPowerSystems and SimDriveline. The PHEV power train is of the series-parallel type (split type), such as the one found in the Toyota Prius car. This PHEV has two kinds of motive power sources: an electric motor and an internal combustion engine (ICE), in order to increase the drive train efficiency and reduce air pollution. It combines the advantages of the electric motor drive (no pollution and high available power at low speed) and the advantages of an internal combustion engine (high dynamic performance and low pollution at high speeds).

The Electrical Subsystem is composed of five parts: The electrical motor, the generator, the battery, the electricity grid connector and the DC/DC converter.

The electrical motor is a 500 Vdc, 50 kW interior Permanent Magnet Synchronous Machine (PMSM) with the associated drive (based on AC6 blocks of the SimPowerSystems Electric Drives library).

This motor has 8 pole and the magnets are buried (salient rotor’s type). A flux weakening vector control is used to achieve a maximum motor speed of 6 000 rpm.

The generator is a 500 Vdc, 2 pole, 30 kW PMSM with the associated drive (based on AC6 blocks of the SimPowerSystems Electric Drives library). A vector control is used to achieve a maximum motor speed of 13000 rpm.

The battery is a 6.5 Ah, 200 Vdc, 21 kW Nickel-Metal-Hydride battery.

The DC/DC converter (boost type) is voltage-regulated. The DC/DC converter adapts the low voltage of the battery (200 V) to the DC bus which feeds the AC motor at a voltage of 500 V.

The Planetary Differential models the power split device. It uses a double planetary device, which transmits the mechanical motive force from the engine, the motor and the generator by allocating and combining them. [14]

The Internal Combustion Engine (ICE) subsystem models a 73 kW @ 5200 rpm gasoline fuel engine with speed governor. The throttle input signal lies between zero and one and specifies the torque demanded from the engine as a fraction of the maximum possible torque. This signal also indirectly controls the engine speed. The engine model does not include air-fuel combustion dynamics.

The Vehicle Dynamics subsystem models all the mechanical parts of the vehicle:

- The single reduction gear reduces the motor’s speed and increases the torque.
- The differential splits the input torque in two equal torques for wheels.
- The tires dynamics represent the force applied to the ground.
- The vehicle dynamics represent the motion influence on the overall system.
- The viscous friction models all the losses of the mechanical system.

The Energy Management Subsystem (EMS) determines the reference signals for the electric motor drive, the electric generator and the internal

combustion engine in order to distribute accurately the power from these three sources. These signals are calculated using mainly the position of the accelerator, which is between -100% and 100%, and the measured PHEV speed. Note that a negative accelerator position represents a positive brake position.

The Battery management system maintains the State-Of-Charge (SOC) between 40 and 80% and “to electricity grid” connection. It prevents against voltage collapse by controlling the power required from the battery. [15]

The Hybrid Management System controls the reference power of the electrical motor by splitting the power demand as a function of the available power of the battery and the generator. The required generator power is achieved by controlling the generator torque and the ICE speed. [16]

There are five main scopes in the model:

- The scope in the Main System named Car shows the accelerator position, the car speed, the drive torque and the power flow.
- The scope in the Drive Electrical Subsystem named PMSM Motor shows the results for the motor drive. You can observe the stator currents i_a , the rotor speed and the motor torque (electromagnetic and reference).
- The scope in the Electrical Subsystem named PMSM Generator shows the results for the generator drive. You can observe the stator

currents i_a , the rotor speed and the motor torque (electromagnetic and reference).

- The scope in the Electrical Subsystem/ Electrical measurements shows the voltages (DC/DC converter, DC bus and battery), the currents (motor, generator and battery) and the battery SOC.
- The scope in the Energy Management Subsystem/Power Management System shows the power references applied to the electrical components.

The general view of the model is shown on Figure 6:

Main System, *Electrical Subsystem* named Motor PMSM, Electrical Subsystem named PMSM Generator DriveElectrical Subsystem/Electrical measurements

Mathematical model of PHEV was developed on the base of MatlabSimulink with the main scopes: Main System, *Electrical Subsystem* named Motor, Electrical Subsystem, Generator DriveElectrical Subsystem and DataMeasurements and Acquisition Subsystem.

User satisfaction criteria

Performances include maximal vehicle velocity, acceleration performances and gradeability. They can be evaluated by simulation in Matlab by following standard approaches described in classical vehicle theory [17, 18].

Maximum speed is evaluated when solving equilibrium equation between propulsion

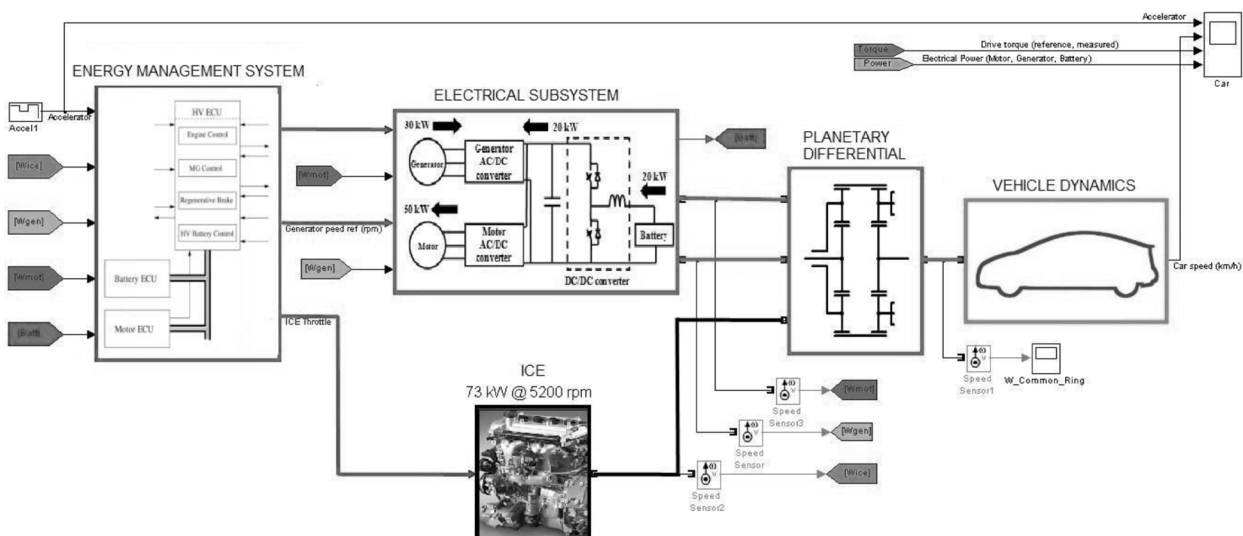


Fig. 6. Matlab based PHEV model.

power and dissipated power by resistance forces (rolling resistance, aerodynamic resistance...)

$$\eta P_{propulsion}(\omega) = P_{resistance}(v) = c_0 v + c_1 v^2 + c_2 v^3 \quad (1)$$

Where ω is engine speed while v is the vehicle ground speed, η is the transmission efficiency, c_0 , c_1 , c_2 - coefficients of a general expression of the driving resistance forces.

Acceleration time (from V_1 to V_2 kph) can be evaluated by solving integration of equation of motion of the vehicle

$$\Delta t = m_{eff} \int_{v_1}^{v_2} \frac{dv}{F_{net}(V)}$$

Where m_{eff} is the equivalent or effective mass and F_{net} , the net force between propulsion force and driving resistance forces.

Gradeability: is estimated by solving the equation limiting the propulsion force that can be transmitted to the ground while taking care of mass transfer during climbing in steady state motion:

$$F_{propulsion} = F_{resistance} \leq \mu W_{f/r}$$

W_f and W_r are respectively the front and rear weight under front or rear wheels.

CONCLUSION

Internal Combustion Engine (ICE) Vehicles need a major change to significantly improve the fuel economy and reduce the emissions. Electric vehicles (EVs) and hybrid EVs (HEVs) have been identified to be the most viable solutions to deal with the problems of ICE fundamentally. Electric drives are the core technology for EVs and HEVs. Among different types of electric drives, there are two major emerging research directions - PM BL

and Induction Motor drive systems. They have been identified and discussed in the paper.

The Energy Management Subsystem (EMS) determines the reference signals for the electric motor drive, the electric generator, the internal combustion engine and battery in order to distribute the power from these sources. Mathematical model of PHEV was developed on the base of Matlab/Simulink with the main scopes: 1) Car - shows the accelerator position, the car speed, the drive torque and the power flow; 2) PMSM Motor and PMSM Generator - for stator currents i_a , rotor speeds and motors torque; 3) Electrical measurements - for the voltages (DC/DC converter, DC bus and battery), the currents (motor, generator and battery) and the battery SOC; 4) Power Management - shows the power references applied to the electrical components.

LITERATURE

1. **Nemry, F.** Plug-in Hybrid and Battery-Electric Vehicles: State of the research and development and comparative analysis of energy and cost efficiency / F. Nemry, G. Leduc, A. Muñoz // European Commission, Joint Research Centre, Institute for Prospective Technological Studies, Luxembourg: Office for Official Publications of the European Communities © European Communities. - 2009.

2. **Plug-in Hybrid Electric Vehicle Definition** / Board of Directors. - 2007. - Mode of access: <http://www.ieeeusa.com/policy/POSITIONS/PHEV0607.pdf>. - Date of access: 24.01.2013.

3. **Meisel, J.** An analytic foundation for the Toyota Prius THS-II powertrain with a comparison to a strong parallel hybrid-electric powertrain / SAE 2006 // World Congress. Detroit, MI. - 2006. - Mode of access: <http://www.toyota.com/prius/specs.html>. - Date of access: 24.01.2013.

4. **Emadi, A.** Power Electronics and Motor Drives in Electric, Hybrid Electric, and Plug-In Hybrid Electric Vehicles / Ali Emadi, Young Joo Lee, Kaushik Rajashekara // IEEE Transactions on

industrial electronics, Vol. 55, No. 6, June 2008. – P.P. 2237 – 2245.

5. **Sun, P.** A 55-kW Three-Phase Inverter Based on Hybrid-Switch Soft-Switching Modules for High-Temperature Hybrid Electric Vehicle Drive Application / Pengwei Sun, Jih-Sheng Lai, Chuang Liu, Wensong Yu // IEEE Transactions on industry applications, Vol. 48, No. 3, May/June 2012. – P.P. 962 – 969.

6. **Lukic, S.** Energy Storage Systems for Automotive Applications / Srdjan M. Lukic, Jian Cao, Ramesh C. Bansal, Fernando Rodriguez, Ali Emadi // IEEE Transactions on industrial electronics, Vol. 55, No. 6, June 2008. – P.P. 2258 – 2267.

7. **Solero, L. L.** Design of multiple-input power converter for hybrid vehicles / L. L. Solero, A. Pomilio, // IEEE Trans. Power Electron., Vol. 20, No. 5, Sep. 2005. - P.P. 1007–1016.

8. **Welchko, B.** Fault Tolerant Three-Phase AC Motor Drive Topologies: A Comparison of Features, Cost, and Limitations / Brian A. Welchko, Thomas A. Lipo, Thomas M. Jahns, Steven E. Schulz // IEEE Transactions on power electronics, Vol. 19, No. 4, July 2004, P.P. 1108 - 1116.

9. **Haddoun, A.** Modeling, Analysis, and Neural Network Control of an EV Electrical Differential / AbdelhakimHaddoun, Mohamed El HachemiBenbouzid, DembaDiallo, RachidAbdessemed, JamelGhouili, KamelSrairi // IEEE Transactions on industrial electronics, Vol. 55, No. 6, June 2008. - P.P. 2286–2294.

10. **Chau, K. T.** Overview of Permanent-Magnet Brushless Drives for Electric and Hybrid Electric Vehicles / K. T. Chau, C. C. Chan, Chunhua Liu // IEEE Transactions on industrial electronics, Vol. 55, No. 6, June 2008. - P.P. 2246–2257.

11. **Лазарев, Ю.Ф.** Начала программирования в среде MATLAB: Учебное пособие.

– К.: НТУУ «КПИ», 2003. – 424 с. – Режим доступа: <http://www.mathworks.com/products/simmechanics>. - Дата доступа: 01.02.2011.

12. **Patrice, B.** Hybrid Electric Vehicle (HEV) Power Train Using Battery Model. – Mode of access: <http://www.mathworks.com/matlabcentral/fileexchange>. Date of access: 24.01.2013.

13. **Marozka, A.A.** Peat briquetting press simulation / A.A.Marozka, Y.N.Petrenko // National and European Dimension in Research. Materials of Junior Researchers' III Conference, Part1, April2011. - P.P. 44-47.

14. **Морозько, О.А.** Имитационная модель автоматизированного электроприводатора фобрикетногопресса / О.А. Морозько, Ю.Н. Петренко // Энергетика... (Изв. высш. учеб. заведений и энерг. объединений СНГ), No. 1, Февраль 2012. - С.С. 30 - 37.

15. **McDonald, D.** Electric Vehicle Drive Simulation with MATLAB/Simulink / David McDonald // LSSU Sault Ste Marie, MI 49783. - Mode of access: dmcDonald@lssu.edu. - Date of access: 03.02.2013.

16. **Design** and Development of Small Electric Vehicle using MATLAB/Simulink // International Journal of Computer Applications, Vol. 24, No.6, June 2011. P.P. 19 – 23.

17. **Kim, M.-J.** Power management and design optimization of fuel cell/battery hybrid vehicles / H. Peng, M.-J. Kim // Journal of Power Sources. - Vol 165, Issue 2. - March 2007. – P.P. 583-593.

18. **Van Mierlo, J.** Comparison of the environmental damage caused by vehicle different alternative fuels and drivetrains in Brussels context / Proceedings of the Institution of Mechanical Engineers // Journal of Automobile Engineering, Part D, 2003. – P.P. 583-593.